

Supplementary Information

Reinvestigation of the spin crossover phenomenon in the ferrous complex $[\text{Fe}(\text{HB(pz)}_3)_2]$

Lionel Salmon,^{a,b*} Gábor Molnár,^{a,b} Saioa Cobo,^{a,b} Pascal Oulié,^{a,b} Michel Etienne,^{a,b} Tarik Mahfoud,^{a,b,c} Philippe Demont,^d Akira Eguchi,^e Hiroshi Watanabe,^e Koichiro Tanaka^e and Azzedine Bousseksou^{a,b*}

^a CNRS, Laboratoire de Chimie de Coordination, 205 route de Narbonne, Toulouse, France

^b Université de Toulouse, UPS, INPT, LCC, 31077 Toulouse, France

^c School of Science and Engineering, Al Akhawayn University in Ifrane, 53000 Ifrane, Morocco

^d Laboratoire de Physique des Polymères-CIRIMAT, CNRS UMR-5085 Université Toulouse III, 118 Route de Narbonne, 31062 Toulouse Cedex, France

^e Department of Physics, Graduate School of Science, Kyoto University, Sakyo-ku, Kyoto 606-8502, Japan

Figure S1. Photographs showing the temperature dependence of the color of the “as prepared” microcrystalline sample $[\text{Fe}(\text{HB(pz)}_3)_2]$ at 295 K (**a**) and at 470 K (**b**) as well as after the first thermal cycle at 295 K (**c**). Microscope images recorded at 295 K displaying the typical aspect of the same sample before (**d**, **e**) and after (**f**, **g**) the first thermal cycle.

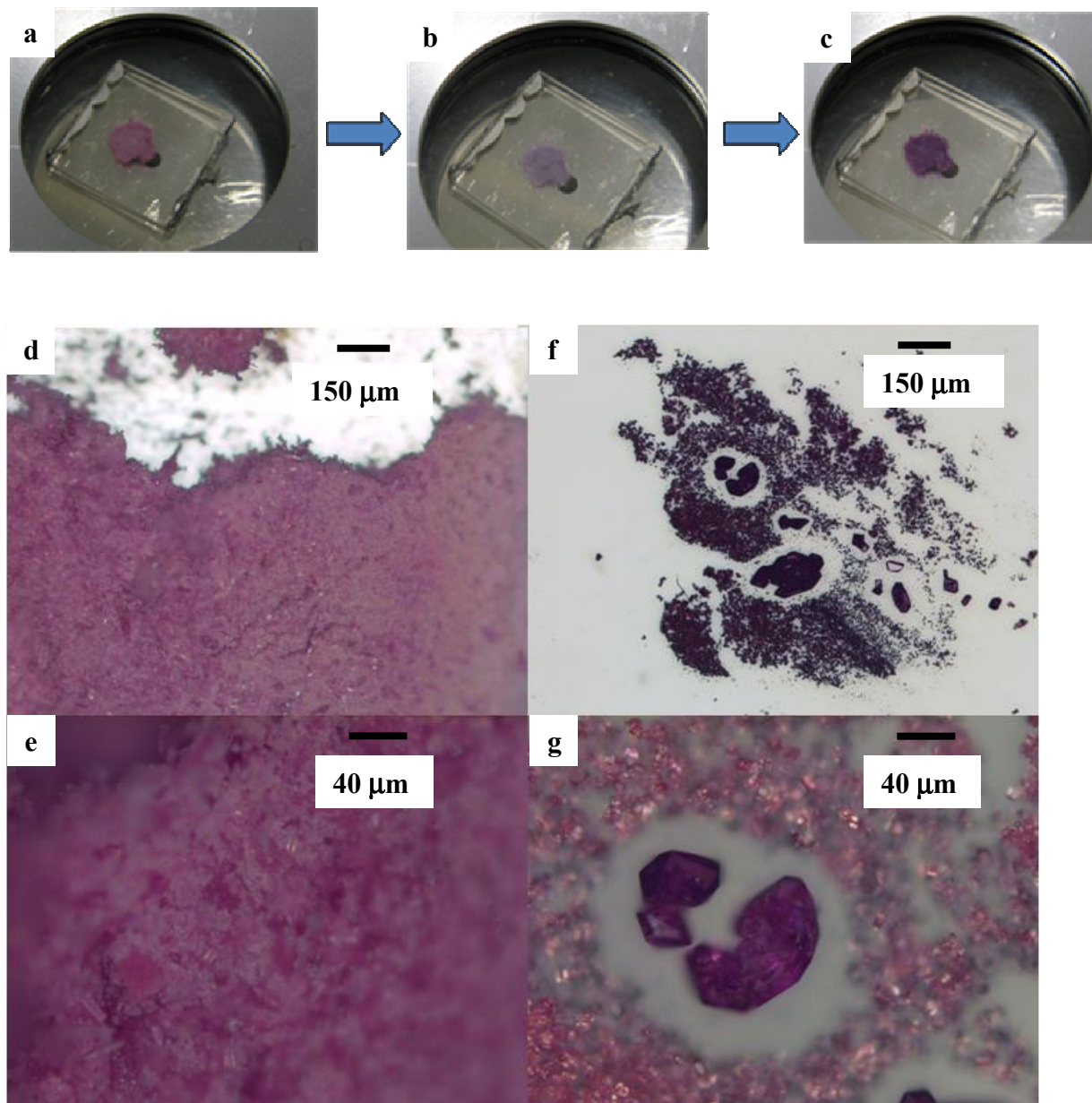


Figure S2. Digital images recorded in-situ during the first heating cycle of **1**.

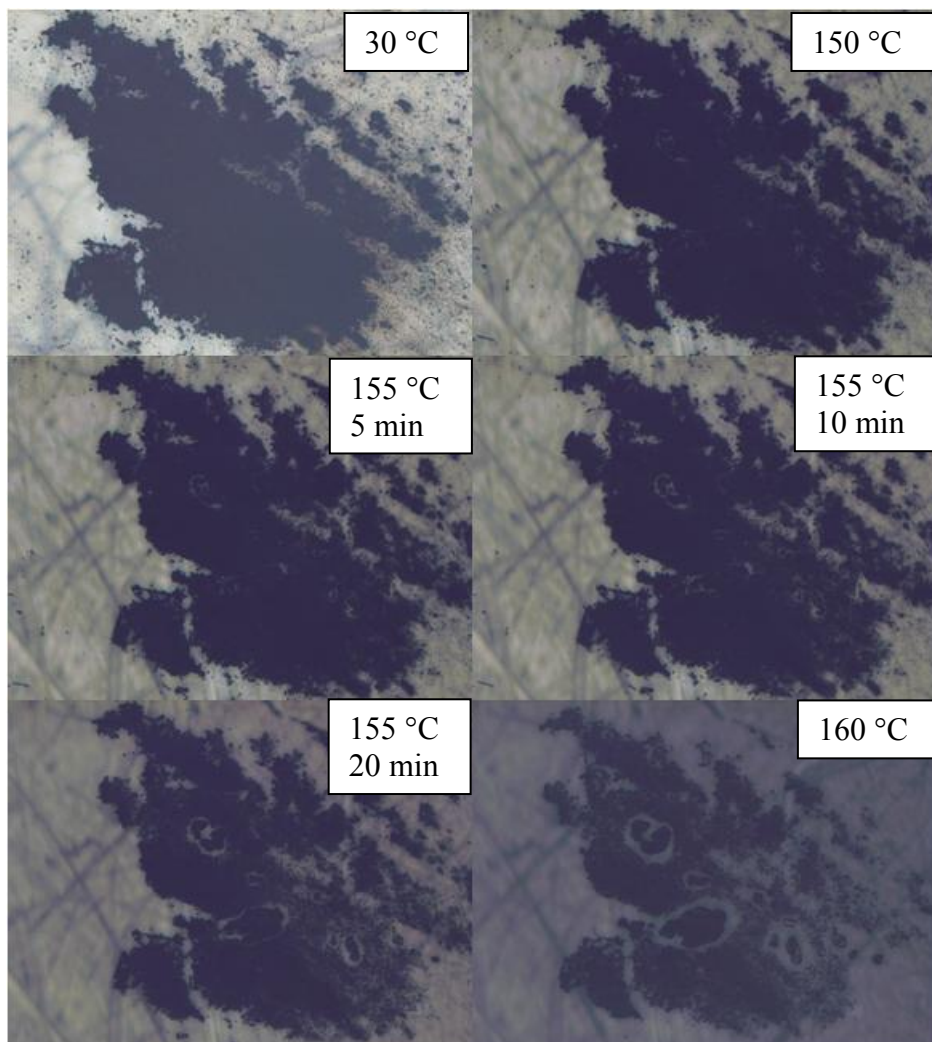
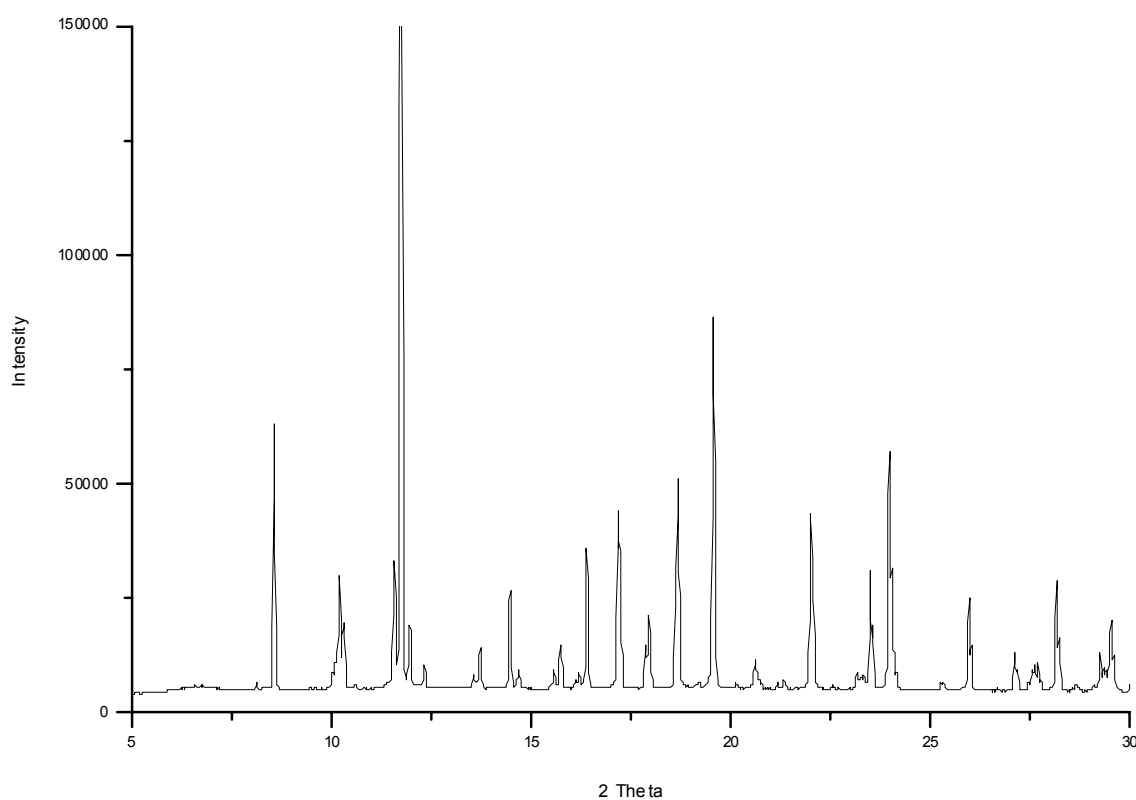


Figure S3. (a) Powder X-ray diffractogram of **1** acquired at 298 K following the first thermal cycle. (b) Powder X-ray diffractogram of **1** calculated from single crystal X-ray data (293 K).

a)



b)

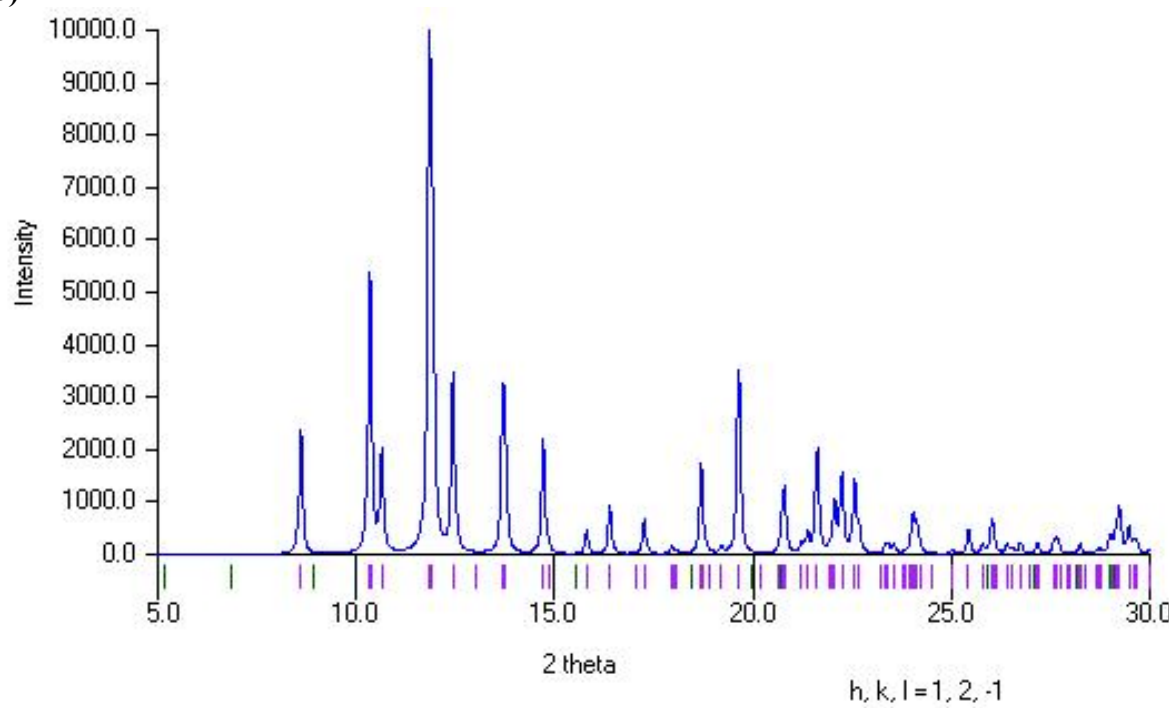


Table S1. Bond distances (\AA) for **1** determined at 298 K and 420 K from single crystal diffraction data

		298 K	420 K
Fe(1)	- N(12)	1.980 (3)	2.095 (4)
Fe(1)	- N(22)	1.987 (3)	2.097 (3)
Fe(1)	- N(32)	1.980 (4)	2.099 (5)
Fe(1)	- N(41)	1.974 (4)	2.091 (5)
Fe(1)	- N(51)	1.992 (3)	2.113 (3)
Fe(1)	- N(61)	1.976 (3)	2.094 (4)
N(11)	- N(12)	1.371 (4)	1.362 (5)
N(11)	- C(11)	1.349 (5)	1.341 (7)
N(11)	- B(1)	1.540 (5)	1.533 (7)
N(12)	- C(13)	1.335 (5)	1.334 (6)
N(21)	- N(22)	1.373 (3)	1.369 (5)
N(21)	- C(21)	1.346 (5)	1.337 (6)
N(21)	- B(1)	1.536 (5)	1.533 (7)
N(22)	- C(23)	1.335 (5)	1.341 (5)
N(31)	- N(32)	1.369 (4)	1.361 (5)
N(31)	- C(31)	1.343 (6)	1.344 (8)
N(31)	- B(1)	1.527 (6)	1.544 (8)
N(32)	- C(33)	1.334 (6)	1.332 (8)
N(41)	- N(42)	1.369 (4)	1.363 (5)
N(41)	- C(41)	1.331 (6)	1.328 (9)
N(42)	- C(43)	1.346 (6)	1.345 (9)
N(42)	- B(2)	1.531 (6)	1.527 (9)
N(51)	- N(52)	1.367 (4)	1.361 (5)
N(51)	- C(51)	1.330 (5)	1.339 (6)
N(52)	- C(53)	1.351 (5)	1.345 (6)
N(52)	- B(2)	1.535 (5)	1.536 (7)
N(61)	- N(62)	1.367 (4)	1.366 (5)
N(61)	- C(61)	1.332 (5)	1.333 (7)
N(62)	- C(63)	1.345 (4)	1.340 (7)
N(62)	- B(2)	1.535 (5)	1.529 (7)
C(11)	- C(12)	1.364 (6)	1.366 (8)
C(12)	- C(13)	1.381 (5)	1.368 (7)
C(21)	- C(22)	1.377 (5)	1.361 (7)
C(22)	- C(23)	1.380 (5)	1.369 (7)
C(31)	- C(32)	1.372 (6)	1.369 (9)
C(32)	- C(33)	1.379 (6)	1.362 (9)
C(41)	- C(42)	1.394 (6)	1.394 (9)
C(42)	- C(43)	1.363 (6)	1.343 (9)
C(51)	- C(52)	1.387 (5)	1.380 (8)
C(52)	- C(53)	1.356 (5)	1.355 (8)
C(61)	- C(62)	1.388 (5)	1.388 (10)
C(62)	- C(63)	1.360 (5)	1.340 (9)

Table S2. Bond angles (deg) for **1** determined at 298 K and 420 K from single crystal diffraction data

			298 K	420 K
N(12)	-	Fe(1)	-	88.33 (11)
N(12)	-	Fe(1)	-	89.05 (12)
N(12)	-	Fe(1)	-	91.67 (12)
N(12)	-	Fe(1)	-	92.68 (11)
N(12)	-	Fe(1)	-	179.01 (12)
N(22)	-	Fe(1)	-	88.35 (12)
N(22)	-	Fe(1)	-	92.25 (12)
N(22)	-	Fe(1)	-	177.97 (12)
N(22)	-	Fe(1)	-	90.88 (11)
N(32)	-	Fe(1)	-	179.07 (13)
N(32)	-	Fe(1)	-	89.91 (12)
N(32)	-	Fe(1)	-	91.53 (12)
N(41)	-	Fe(1)	-	89.48 (12)
N(41)	-	Fe(1)	-	87.75 (12)
N(51)	-	Fe(1)	-	88.12 (11)
N(12)	-	N(11)	-	109.1 (3)
N(12)	-	N(11)	-	118.0 (2)
C(11)	-	N(11)	-	132.7 (3)
Fe(1)	-	N(12)	-	119.3 (2)
Fe(1)	-	N(12)	-	134.3 (2)
N(11)	-	N(12)	-	106.0 (3)
N(22)	-	N(21)	-	109.6 (3)
N(22)	-	N(21)	-	118.4 (2)
C(21)	-	N(21)	-	132.0 (3)
Fe(1)	-	N(22)	-	118.74 (19)
Fe(1)	-	N(22)	-	135.5 (2)
N(21)	-	N(22)	-	105.7 (3)
N(32)	-	N(31)	-	109.5 (3)
N(32)	-	N(31)	-	117.7 (3)
C(31)	-	N(31)	-	132.7 (3)
Fe(1)	-	N(32)	-	119.8 (3)
Fe(1)	-	N(32)	-	134.2 (2)
N(31)	-	N(32)	-	105.9 (3)
Fe(1)	-	N(41)	-	119.1 (3)
Fe(1)	-	N(41)	-	134.9 (2)
N(42)	-	N(41)	-	106.0 (3)
N(41)	-	N(42)	-	108.9 (3)
N(41)	-	N(42)	-	118.6 (3)
C(43)	-	N(42)	-	132.3 (3)
Fe(1)	-	N(51)	-	119.2 (2)
Fe(1)	-	N(51)	-	134.2 (2)
N(52)	-	N(51)	-	106.1 (3)
N(51)	-	N(52)	-	109.2 (3)
N(51)	-	N(52)	-	118.2 (2)
C(53)	-	N(52)	-	132.0 (3)
Fe(1)	-	N(61)	-	119.9 (2)
Fe(1)	-	N(61)	-	134.2 (2)
N(62)	-	N(61)	-	105.8 (3)
N(61)	-	N(62)	-	109.8 (3)
N(61)	-	N(62)	-	117.7 (2)
C(63)	-	N(62)	-	132.5 (3)
N(11)	-	C(11)	-	108.8 (3)
C(11)	-	C(12)	-	105.1 (4)
N(12)	-	C(13)	-	110.9 (3)

N (21)	-	C (21)	-	C (22)	108.5 (3)	108.7 (4)
C (21)	-	C (22)	-	C (23)	104.9 (3)	105.3 (4)
N (22)	-	C (23)	-	C (22)	111.3 (3)	111.0 (3)
N (31)	-	C (31)	-	C (32)	108.6 (3)	108.3 (5)
C (31)	-	C (32)	-	C (33)	105.0 (4)	105.1 (5)
N (32)	-	C (33)	-	C (32)	111.0 (3)	111.5 (5)
N (41)	-	C (41)	-	C (42)	111.3 (3)	111.1 (5)
C (41)	-	C (42)	-	C (43)	104.0 (4)	104.1 (6)
N (42)	-	C (43)	-	C (42)	109.7 (3)	110.2 (5)
N (51)	-	C (51)	-	C (52)	110.7 (3)	110.5 (5)
C (51)	-	C (52)	-	C (53)	105.3 (3)	105.5 (4)
N (52)	-	C (53)	-	C (52)	108.6 (3)	108.5 (4)
N (61)	-	C (61)	-	C (62)	110.7 (3)	111.3 (5)
C (61)	-	C (62)	-	C (63)	105.3 (3)	104.2 (5)
N (62)	-	C (63)	-	C (62)	108.5 (3)	110.2 (5)
N (11)	-	B (1)	-	N (21)	106.8 (3)	109.1 (4)
N (11)	-	B (1)	-	N (31)	109.1 (3)	109.2 (4)
N (21)	-	B (1)	-	N (31)	107.7 (3)	108.0 (4)
N (42)	-	B (2)	-	N (52)	108.2 (3)	109.6 (4)
N (42)	-	B (2)	-	N (62)	108.1 (3)	109.7 (4)
N (52)	-	B (2)	-	N (62)	106.8 (3)	107.9 (4)

Table S3. Variation of the unit cell parameters of the powder sample of **1** during the first heating sequence

	298 K	318 K	338 K	358 K	378 K	398 K	413 K	variation
a (Å)	17.11	17.11	17.166	17.190	17.242	17.31	17.37	+1.520%
b (Å)	17.11	17.11	17.166	17.190	17.242	17.31	17.37	+1.520%
c (Å)	7.493	7.496	7.520	7.544	7.565	7.563	7.567	+0.988%
α (deg)	90	90	90	90	90	90	90	-
β (deg)	90	90	90	90	90	90	90	-
γ (deg)	90	90	90	90	90	90	90	-
V (Å ³)	2194.4	2194.6	2216.0	2229.2	2249.0	2265.5	2282.6	+4.019%